Published in final edited form as:

J Immunol. 2018 July 15; 201(2): 337–342. doi:10.4049/jimmunol.1800279.

Evidence for non-vascular route of visceral organ immunosurveillance by T cells

Elizabeth M Steinert[*,‡,§], **Emily A Thompson**[*,§], **Lalit K Beura**[*], **Omar A Adam**[*], **Jason S Mitchell**[†], **Mengdi Guo**[*,¶], **Elise R Breed**[†], **Frances V Sjaastad**[*], **Vaiva Vezys**[*], and **David Masopust**[*]

[*]Center for Immunology, Department of Microbiology and Immunology, University of Minnesota, Minneapolis, MN 55455

[†]Center for Immunology, Department of Lab Medicine and Pathology, University of Minnesota, Minneapolis, MN 55455

Abstract

Lymphocytes enter tissues from blood vessels through a well-characterized three-step process of extravasation. To our knowledge, non-vascular routes of lymphocyte entry have not been described. In mice, here we report that Ag-experienced CD8 T cells recirculate from blood through the peritoneal cavity. In the event of infection, Ag-experienced CD8 T cell subsets adhered to visceral organs, indicating potential transcapsular immunosurveillance. Focusing on the male genital tract (MGT), we observed Ag-experienced CD8 T cell migration from the peritoneal cavity directly to the infected MGT across the capsule, which was dependent on the extracellular matrix receptor CD44. We also observed that following clearance of infection, the MGT retained functional resident memory CD8 T cells. These data suggest that recirculation through body cavities may provide T cells with opportunities for broad immunosurveillance and potential non-vascular mechanisms of entry.

Introduction

T cells migrate into tissues from blood vessels using canonical three-step selectin, chemokine, and integrin dependent pathways (1, 2). Migration is selective and changes with T cell differentiation state (3). Naïve T cells recirculate amongst secondary lymphoid organs (SLO). During an immunological insult, activated T cells leave lymphoid tissue and gain the ability to extravasate across post capillary venules and into non-lymphoid tissue (NLT) where they scan host cells for evidence of foreign Ag. If Ag is cleared, three different expanded populations of memory T cells remain (4). T_{CM} cells recirculate between blood and SLO whereas T_{EM} cells recirculate through blood and putatively through NLT. Recirculation occurs by entering tissues via blood vessels and egressing via lymphatic

Address correspondence to Dr. David Masopust, University of Minnesota, 2101 6th Street SE, Minneapolis, MN 55455. Phone: 612-625-4666, masopust@umn.edu.

[‡]Current: Department of Medicine, Northwestern University Feinberg School of Medicine, Chicago, IL, 60611

[¶]Current: Department of Immunology, University of Toronto, Toronto, Ontario, Canada

[§]Authors contributed equally to this work

vessels. The third memory T cell population, tissue resident memory T cells (T_{RM}), surveys tissues without recirculating. T_{RM} represent the dominant subset that patrols NLT (5, 6). Importantly, T_{RM} appear to be first line responders in the case of reinfections at barrier and mucosal sites (7–12).

The MGT is a major site of transmission and acquisition of sexually transmitted infections (STI). Compared to many NLT, including the FRT, memory CD8 T cell mediated immunosurveillance of the MGT is poorly characterized due to technical limitations. Unlike most mucosal sites, the MGT is considered to be immune-privileged. Transplant studies have demonstrated the immune-privilege of the testes both as a transplant tissue, and transplant site (13, 14). Mechanisms of immune privilege in the testes are necessary because developmentally regulated germ cell Ags are highly immunogenic. These mechanisms are predominantly carried out by Sertoli cells and include both physical and molecular barriers. For example, tight junctions between Sertoli cells establish a blood-testis barrier, while their expression of FasL has been shown to eliminate immune cells that pose a threat to germ cells and developing sperm (15–19). Type 2 macrophages, TGFβ, IL-10 production and altered MHC expression also contribute to an immunosuppressive environment in the testes (13, 20–22).

Given the immune-privileged status of the MGT and potential implications for STI vaccination, we tested whether T_{RM} CD8 T cells could be established at this site. During the course of these investigations, we observed an unexpected mechanism for T cell migration to the MGT, which may have broad ramifications for immunosurveillance of visceral organs.

Material and Methods

Mice, adoptive transfers and infections

Mice were used in accordance with the Institutional Animal Care and Use Committee at the University of Minnesota. C57BL/6J and CD44KO mice were purchased from The Jackson Laboratory, P14 and OT-I CD8 T cell transgenic mice were maintained in house. For endogenous studies naïve C57BL/6J mice were infected with 2×10^5 PFU LCMV Armstrong i.p. P14 immune chimeras were generated by transferring 5×10^4 naïve P14 CD8 T cells into naïve C57BL/6J mice, one day prior to i.p. infection with 2×10^5 PFU LCMV. OT-I effector cells were generated by transferring 5×10^4 naive OT-I CD8 T cells into naïve C57BL/6J mice one day prior to i.v. infection with 1×10^6 PFU VSV-OVA. Influenza experiments were conducted by transferring 5×10^4 naïve P14 CD8 T cells into naïve C57BL/6J mice one day prior to intranasal inoculation with 3.4×10^4 PFU (1000 $TCID_{50}$) flu-gp33. Pet store mice were acquired and housed as described (23).

Transurethral instillation

Transurethral instillations were performed as previously described (24).

Isolations, *ex vivo* peptide stimulations & flow cytometry

In vivo i.v. antibody staining and isolation of lymphocytes from peripheral blood, spleen, LN, SG and SI was performed as described (5, 25). Lymphocytes were isolated from MGT

using published methods for SG (5). For *ex vivo* re-stimulation, single cell suspensions were incubated with 0.2μg/ml gp33 peptide or control media for 4h at 37C.

Tissue freezing, immunofluorescence and microscopy

Fixed or fresh frozen tissues were prepared as described (5, 10, 23). Quantitative immunofluorescence microscopy (QIM) performed as described (5, 10).

Two-photon laser scanning microscopy

A Leica TCS MP resonance-scanning microscope with two nondescanned photomultiplier detectors, two HyD detectors and a Mai Tai DeepSee two-photon laser (15 W; Spectra-Physics) at 920 nm was used to excite samples for imaging. Explants were immobilized on coverslips, and kept at 37C with circulating RPMI 1640 media bubbled with 95% O_2 5% CO_2. The *x*-*y* acquisition dimensions were 256 × 256μm and were scanned at 8000 Hz. Z-stacks of 100–150μm at a 2.5μm step size were acquired every 30 seconds for 30-45 min. Imaris 8.1×64 software was used for analysis (Bitplane).

Results & Discussion

Resident-phenotype memory CD8 T cells persist in male genital tract

We first tested whether a model viral infection, lymphocytic choriomeningitis virus (LCMV, Armstrong strain), infected the MGT, and then addressed whether the MGT was amenable to the establishment of memory CD8 T cells. Naïve C57Bl/6J mice received naïve LCMV-specific (for the gp_{33-41} epitope) P14 CD8 T cells i.v., and were infected the following day with 2×10^5 pfu LCMV i.p. Four days later, LCMV was detected in MGT tissues as well as spleen and other visceral organs (Fig. 1A & data not shown). P14 CD8 T cells began to infiltrate the MGT by seven days after infection (Fig. 1B), when they were concentrated near the tissue capsule. In contrast, after viral clearance, the remaining memory P14 cell population was evenly distributed throughout MGT tissues. Quantitative immunofluorescence microscopy (QIM) revealed that the frequency of Ag-specific memory CD8 T cells per million nucleated host cells in MGT was comparable to other organs and the FRT of LCMV-immune female mice (Fig. 1C). P14 cells also bore CD69 and CD103, markers of T_{RM}, and produced IFNγ, but not TNFα 12h after *in vivo* transurethral instillation of cognate (gp_{33-41}) peptide (Fig. 1D-G & Supplemental Fig 1A). Distribution of CD103+ and CD103− CD69+ cells was similar to LCMV-specific T_{RM} isolated from the female reproductive tract (5, 26). A similar trend was observed upon *in vitro* activation with normalized numbers of splenic feeder cells (Supplemental Fig. 1B-C). Direct tissue infection was not required for memory CD8 T cell establishment because intranasal infection with recombinant influenza A/PR/8/34 virus expressing gp_{33-41} (flu-gp33) also established memory P14 cells within the MGT (Supplemental Fig. 2A). CD8β+ T cells were also found throughout the MGT of pet store mice, which have an extensive infectious history (Supplemental Fig. 2B). Because these mice had recently fathered litters, these findings suggest that CD8β+ T cell populations are maintained in MGT tissues under normal circumstances and did not abrogate the mouse's ability to procreate.

Transcapsular effector CD8 T cell migration

The capsular localization of effector CD8 T cells early after infection led us to ask if P14 cells might migrate directly into the MGT from the peritoneal cavity. We isolated P14 cells from lymphoid tissues of immune chimeras 6 days after LCMV infection (Day 6 effector P14 cells), mixed them with congenically marked naïve P14 CD8 T cells and transferred this mixture of effector and naïve P14 CD8 T cells, i.p. to day 6 LCMV infection-matched recipients. Three hours later, tissues were harvested and analyzed for migration of effector and naïve P14 CD8 T cells. Immunofluorescence revealed that effector P14 CD8 T cells from immune chimeras infected 6 days prior were adhered to the capsule of visceral organs including the testes and epididymis and appeared to be migrating across the outermost cell layers of these organs (Fig. 2A-C). We next used 2-photon microscopy to determine if the day 6 effectors simply adhered to the tissues or were in fact migrating across the capsule. Effector P14 CD8 T cells were visualized and recorded moving below the superficial collagen layers of the testes and epididymis. Two-dimensional (YZ) flattened still images (of 2-photon movies) show a cell fully encircled by collagen while two other cells are adhered to the surface nearby (Fig. 2D & Supplemental Video 1). The motility of the migrated CD8 T cells below the collagen layer demonstrates viability of cells that have undergone transcapsular migration (Data not shown, Supplemental Video 1).

To verify that transcapsular migration was indeed independent of canonical lymphocyte migration from blood vessels, day 6 effector P14 CD8 T cells were harvested and co-incubated *in vitro* for 2-3h with organs from infection-matched hosts. Following incubation, day 6 effector P14 CD8 T cells were observed by 2-photon microscopy to have migrated into the tissue (Fig. 2E & Supplemental Video 2). Further, peripheral blood (PBL) was taken at the time of sacrifice after 3h *in vivo* incubation (as in Fig 2A-D) and was absent of i.p. injected cells, indicating that they do not access blood within 3h. This was confirmed with a time course of PBL wherein effector and naïve CD8 T cells finally arrived in PBL 12h after i.p. injection (Fig. 2F). Thus, effector and naïve P14 CD8 T cells had not yet arrived in PBL during the 3h *in vivo* incubation during which transcapsular migration had occurred. Adherence and migration was limited to recently infected tissue, because 3h after i.p. injection, effector P14 cells from a day 6 post infection LCMV mouse were only adhered to the visceral organs of an infection-matched, but not naïve recipient (Fig. 2G). Effector P14 cells were also observed adhered to other visceral organs from infection-matched recipients, such as spleen and kidney (Fig. 2H). Taken together, these data indicate that peritoneal CD8 T cells have the capacity to adhere to infected visceral organs, and to migrate subjacent to collagen and cytokeratin-dense tissue capsule.

Recirculation through peritoneal cavity by memory CD8 T cells allows adherence and transcapsular migration to infected MGT

It is well known that lymphocytes injected into the peritoneal cavity of uninfected mice will eventually join the recirculating pool in blood. We wondered if non-vascular routes of tissue migration might be used by memory CD8 T cells performing immunosurveillance of visceral organs via peritoneal recirculation. Memory CD8 T cells from peritoneal lavage predominantly lack CD69 and CD103 markers of tissue residence, unlike P14 T_{RM} isolated from small intestine epithelium (Fig. 3A). Eighteen hours after i.v. transfer of memory P14

CD8 T cells isolated from spleen, both T_{CM} (CD62L+) and T_{EM} (CD62L-) P14 cells were isolated from peritoneal lavage (Fig. 3B). This suggests that in addition to secondary lymphoid organs, blood, and lymphatic vessels, that T_{CM} and T_{EM} constitutively recirculate through the peritoneal cavity during the course of routine surveillance.

In an intact response, it is not possible to discriminate between cells migrating via blood versus those undergoing transcapsular migration, thus the contribution of transcapsular migration to an immune response cannot be directly gauged. However, because memory CD8 T cells recirculate through the peritoneal cavity, and thus might perform immunosurveillance via transcapsule migration, we asked if they would adhere to recently infected tissue at the same rate as effector P14 cells. To this end we co-transferred congenically marked naïve, effector, and memory P14 cells into recipients infected 6 days prior with LCMV (Fig. 3C). Adherence of effector and memory P14 cells to infection-matched tissues was not significantly different, while naïve P14 CD8 T cells failed to adhere to recently infected tissue. 2-photon imaging of explants co-cultured for 3h revealed that memory P14 CD8 T cells were capable of both attaching (Not Embedded, and associated with rolling) and also entering tissue (Embedded) as evidenced by three-dimensional analyses showing cells unequivocally beneath the capsule (Fig. 3D & Supplemental Video 3). Some regions appeared to be dominated by attached cells, and others by embedded cells, although the basis for this variance is unclear and embedded cells were difficult to quantify.

Antigen-independent, CD44-dependent mechanism of visceral immunosurveillance

Visceral attachment depended on recent infection of the host. To determine if local cognate Ag recognition was required, we co-transferred effector OT-I (primed 6 days prior *in vivo* with recombinant VSV expressing ovalbumin, VSV-OVA) and P14 CD8 T cells (primed against LCMV) i.p. into recipients infected 6 days earlier with LCMV (these mice would not present the ovalbumin peptide recognized by OT-I). Three hours later, attached P14 and OT-I cells were enumerated in testes and epididymis, which indicated that local Ag recognition is not absolutely required (Fig. 4A). While the difference in attachment between Ag-specific and non-specific populations appears substantial, it fails to reach significance and may be a result of the different viral infections (VSV-OVA vs. LCMV) used to generate the day 6 post infection effector cells. In contrast, when effector P14 cells were incubated with pertussis toxin and injected i.p. into day 6 infection-matched recipients, attachment appeared compromised, suggesting involvement of chemokine receptor signaling (Fig. 4B).

During the course of our investigations, a study reported direct migration of peritoneal resident macrophages into damaged liver, and indicated a requirement for CD44, which binds hyaluronan (27). We quantified adherence of day 6 effector CD8β+ T cells from either CD44KO or WT mice 3h after i.p. transfer into infection-matched recipients. As seen in figure 4C, CD44KO CD8β+ T cells adhered significantly less than WT counterparts. To confirm this mechanism with an Ag-specific T cell population, we i.p. injected untreated or anti-CD44 antibody treated effector P14 cells into either untreated or hyaluronidase-treated infection-matched recipients, respectively. Anti-CD44 and hyaluronidase treatment significantly diminished P14 cell tissue adherence and transcapsular migration (Fig. 4D).

This study provides evidence for a nonvascular, transcapsular pathway of migration by Ag-experienced T cells within infected mice. This noncanonical lymphocyte migration pathway may bear some relation to migration of peritoneal resident macrophages into damaged liver, because both processes required CD44 (27).

To speculate, our findings suggest an efficient means of immunosurveillance of visceral organs. These results might have implications for understanding immunosurveillance of the pleural cavity as well. Future studies are needed to assess the role of this migration process in protection against or control of infections, cancer metastases or immunosurveillance, and the long-term fate of transcapular migrants including whether they contribute to stromal tissue resident memory T cells.

Supplementary Material

Refer to Web version on PubMed Central for supplementary material.

Acknowledgments

This work was supported by: NIH Grant R01AI111671 and R01AI084913 (to D.M.); University of Minnesota Doctoral Dissertation Fellowship (to E.M.S. and E.A.T.)

Abbreviations

MGT	male genital tract
FRT	female reproductive tract
SG	salivary gland
LN	lymph node
SI	small intestine
IEL	intraepithelial lymphocyte
LCMV	lymphocytic choriomeningitis virus
T_{CM}	central memory
T_{EM}	effector memory
T_{RM}	tissue-resident memory
VSV	vesicular stomatitis virus

References

1. von Andrian UH, Mackay CR. T-Cell Function and Migration — Two Sides of the Same Coin. N Engl J Med. 2000; 343:1020–1034. [PubMed: 11018170]
2. Butcher EC, Picker LJ. Lymphocyte homing and homeostasis. Science. 1996; 272:60. [PubMed: 8600538]
3. Masopust D, Schenkel JM. The integration of T cell migration, differentiation and function. Nat Rev Immunol. 2013; 13:309–320. [PubMed: 23598650]

4. Mueller SN, Gebhardt T, Carbone FR, Heath WR. Memory T cell subsets, migration patterns, and tissue residence. Annu Rev Immunol. 2013; 31:137–161. [PubMed: 23215646]
5. Steinert EM, Schenkel JM, Fraser KA, Beura LK, Manlove LS, Igyártó BZ, Southern PJ, Masopust D. Quantifying memory CD8 T cells reveals regionalization of immunosurveillance. Cell. 2015; 161:737–749. [PubMed: 25957682]
6. Farber DL, Yudanin NA, Restifo NP. Human memory T cells: generation, compartmentalization and homeostasis. Nat Rev Immunol. 2014; 14:24–35. [PubMed: 24336101]
7. Park CO, Kupper TS. The emerging role of resident memory T cells in protective immunity and inflammatory disease. Nat Med. 2015; 21:688–697. [PubMed: 26121195]
8. Teijaro JR, Turner D, Pham Q, Wherry EJ, Lefrançois L, Farber DL. Cutting edge: Tissue-retentive lung memory CD4 T cells mediate optimal protection to respiratory virus infection. J Immunol. 2011; 187:5510–5514. [PubMed: 22058417]
9. Gebhardt T, Wakim LM, Eidsmo L, Reading PC, Heath WR, Carbone FR. Memory T cells in nonlymphoid tissue that provide enhanced local immunity during infection with herpes simplex virus. Nat Immunol. 2009; 10:524–530. [PubMed: 19305395]
10. Schenkel JM, Fraser KA, Vezys V, Masopust D. Sensing and alarm function of resident memory CD8+ T cells. Nat Immunol. 2013; 14:509–513. [PubMed: 23542740]
11. Ariotti S, Hogenbirk MA, Dijkgraaf FE, Visser LL, Hoekstra ME, Song JY, Jacobs H, Haanen JB, Schumacher TN. Skin-resident memory CD8+ T cells trigger a state of tissue-wide pathogen alert. Science. 2014; 346:101–105. [PubMed: 25278612]
12. Stary G, Olive A, Radovic-Moreno AF, Gondek D, Alvarez D, Basto PA, Perro M, Vrbanac VD, Tager AM, Shi J, Yethon JA, Farokhzad OC, Langer R, Starnbach MN, von Andrian UH. A mucosal vaccine against Chlamydia trachomatis generates two waves of protective memory T cells. Science. 2015; 348
13. Meinhardt A, Hedger MP. Immunological, paracrine and endocrine aspects of testicular immune privilege. Mol Cell Endocrinol. 2011; 335:60–68. [PubMed: 20363290]
14. Setchell BP. The testis and tissue transplantation: historical aspects. J Reprod Immunol. 1990; 18:1–8.
15. Chiquoine AD. Observations on the early events of cadmium necrosis of the testis. Anat Rec. 1964; 149:23–35. [PubMed: 14158504]
16. Brökelmann J. Fine structure of germ cells and Sertoli cells during the cycle of the seminiferous epithelium in the rat. Z Für Zellforsch Mikrosk Anat. 1963; 59:820–850.
17. Flickinger CJ. The postnatal development of the Sertoli cells of the mouse. Z Fuer Zellforsch Mikrosk Anat. 1967; 78:92–113.
18. Flickinger C, Fawcett DW. The junctional specializations of Sertoli cells in the seminiferous epithelium. Anat Rec. 1967; 158:207–221. [PubMed: 6034643]
19. Nicander L. An electron microscopical study of cell contacts in the seminiferous tubules of some mammals. Z Für Zellforsch Mikrosk Anat. 1967; 83:375–397.
20. Suarez-Pinzon W, Korbutt GS, Power R, Hooton J, Rajotte RV, Rabinovitch A. Testicular sertoli cells protect islet beta-cells from autoimmune destruction in NOD mice by a transforming growth factor-beta1-dependent mechanism. Diabetes. 2000; 49:1810–1818. [PubMed: 11078447]
21. O'Bryan MK, Gerdprasert O, Nikolic-Paterson DJ, Meinhardt A, Muir JA, Foulds LM, Phillips DJ, de Kretser DM, Hedger MP. Cytokine profiles in the testes of rats treated with lipopolysaccharide reveal localized suppression of inflammatory responses. Am J Physiol - Regul Integr Comp Physiol. 2005; 288:R1744–R1755. [PubMed: 15661966]
22. Pöllánen P, Niemi M. Immunohistochemical identification of macrophages, lymphoid cells and HLA antigens in the human testis. Int J Androl. 1987; 10:37–42. [PubMed: 3294605]
23. Beura LK, Hamilton SE, Bi K, Schenkel JM, Odumade OA, Casey KA, Thompson EA, Fraser KA, Rosato PC, Filali-Mouhim A, Sekaly RP, Jenkins MK, Vezys V, Haining WN, Jameson SC, Masopust D. Normalizing the environment recapitulates adult human immune traits in laboratory mice. Nature. 2016; 532:512–516. [PubMed: 27096360]
24. Boehm BJ, Colopy SA, Jerde TJ, Loftus CJ, Bushman W. Acute bacterial inflammation of the mouse prostate. The Prostate. 2012; 72:307–317. [PubMed: 21681776]

25. Anderson KG, Mayer-Barber K, Sung H, Beura L, James BR, Taylor JJ, Qunaj L, Griffith TS, Vezys V, Barber DL, et al. Intravascular staining for discrimination of vascular and tissue leukocytes. Nat Protoc. 2014; 9:209–222. [PubMed: 24385150]

26. Casey KA, Fraser KA, Schenkel JM, Moran A, Abt MC, Beura LK, Lucas PJ, Artis D, Wherry EJ, Hogquist K, et al. Antigen-independent differentiation and maintenance of effector-like resident memory T cells in tissues. J Immunol. 2012; 188:4866–4875. [PubMed: 22504644]

27. Wang J, Kubes P. A Reservoir of Mature Cavity Macrophages that Can Rapidly Invade Visceral Organs to Affect Tissue Repair. Cell. 2016; 165:668–678. [PubMed: 27062926]

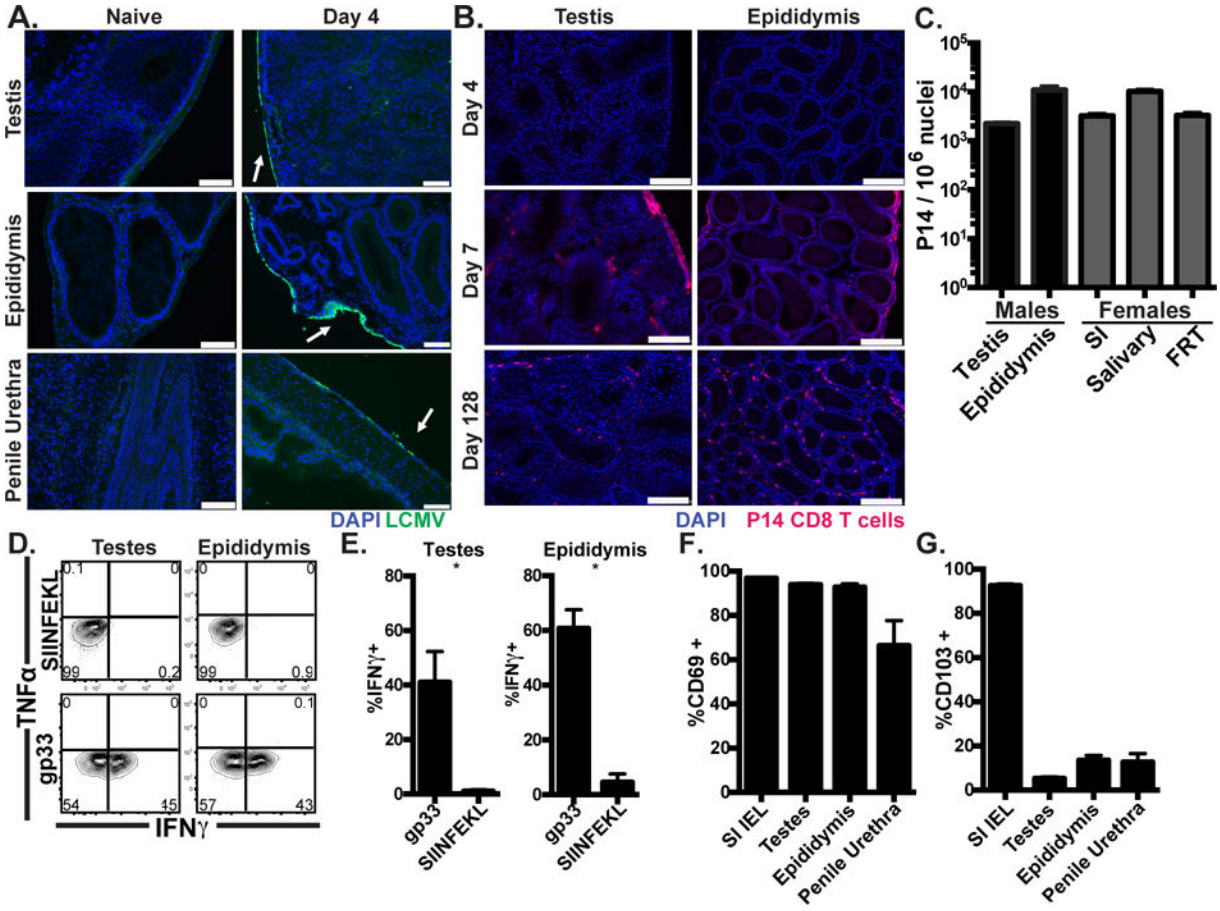

FIGURE 1. Resident-phenotype memory CD8 T cells persist in male genital tract

(A) C57BL/6 mice were infected with LCMV i.p. and stained with anti-LCMV nucleoprotein antibody (Green), and DAPI (Blue). Scale bar=100μm. n=8 from 3 experiments. (B) Representative images 4, 7 or 128 days after Thy1.1+ P14 cell transfer and LCMV infection, Thy1.1+ P14 (red), DAPI (Blue), scale bar=250μm, n=6-8 from 2 or 3 experiments per time point. (C) Enumeration of Thy1.1+ P14 in tissues from male (black) or age-matched female (grey) mice 115-160 days after LCMV infection, n=6, representative of 4 experiments. (D-E) 120-160 days after LCMV infection, 50μg of gp33 (cognate) or SIINFEKL (irrelevant) peptide was transurethrally instilled. 12h later, P14 were isolated and cytokine expressing cells were assessed by flow cytometry. n=6, representative of 3 experiments. (F-G) CD69 and CD103 expression on P14 memory cells, n=12 from 3 experiments. Graphs show mean and SEM, *p 0.0357, Mann-Whitney.

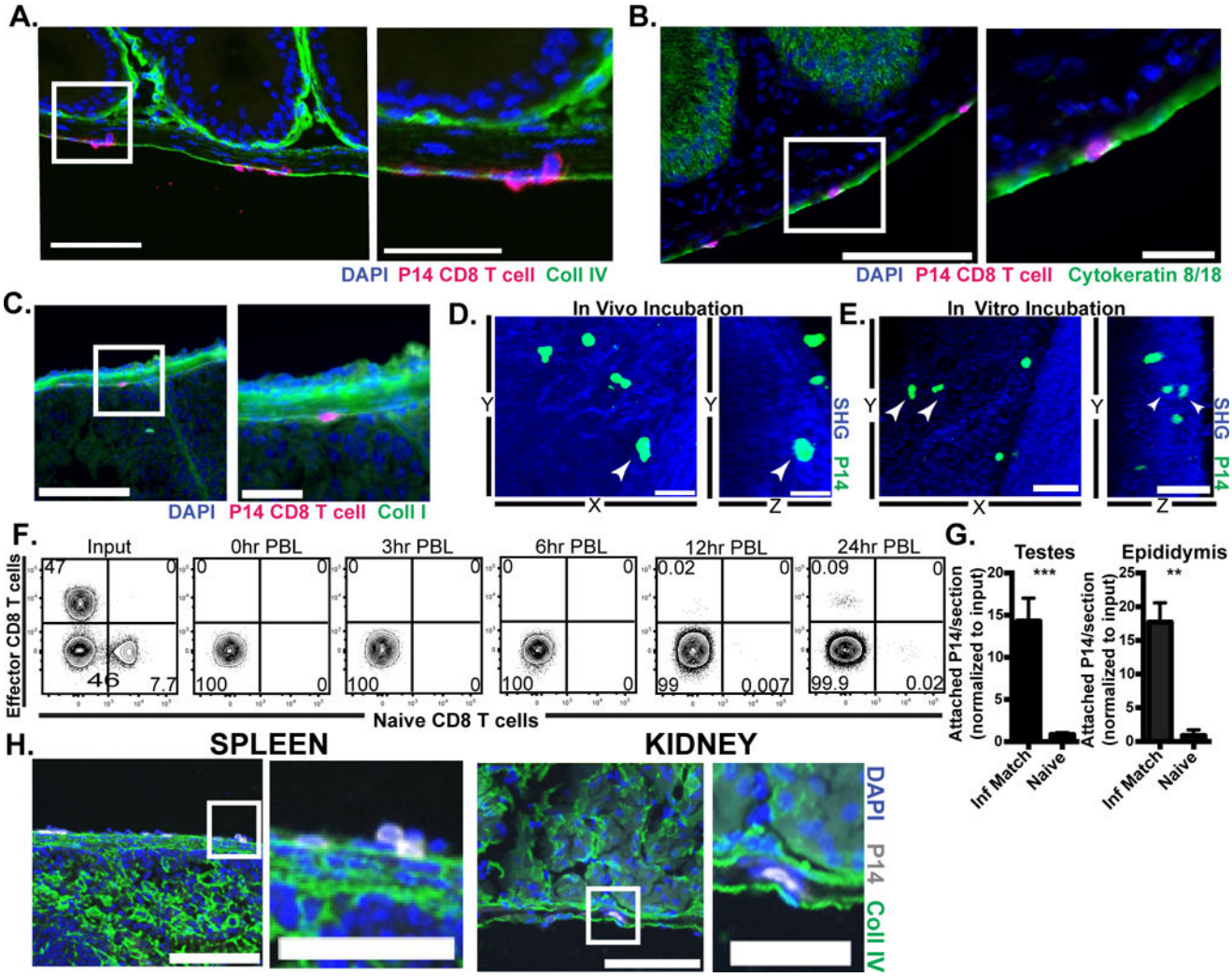

FIGURE 2. Evidence that effector CD8 T cells enter visceral tissues via direct transcapsular migration

0.5-1×10^6 CD45.1+ naïve P14 CD8 T cells and 3-4×10^6 Thy1.1+ effector P14 from mice infected with LCMV 6 days prior (D6 effector) were mixed and co-transferred i.p. into day 6 LCMV infection-matched recipients. 3h after injection tissues were harvested and analyzed for migration of transferred cells. (A-C) Representative images of adhered and migrating effector P14 CD8 T cells (in magenta) on epididymis, DAPI (in blue) indicates nuclei. Part of the section on the left (white rectangle) is shown in higher magnification in the right. Scale bars=100μm (left panels) and 25μm (right panels). Sections were also stained for stromal markers (in green) including (A) collagen IV, (B) cytokeratin 8 and 18, and (C) collagen I. (D) 3-4×10^6 LCMV D6 effector P14-gfp were i.p. transferred to infection-matched recipients. 3h after injection, the MGT was harvested and P14-gfp attachment was evaluated using 2-photon microscopy. Still images from 2-photon microscopy video show a P14 CD8 T cell (white arrowhead) under the collagen capsule layer, third dimension is flattened. Scale bar=30μm (left, *in vivo* panel). (E) 4×10^6 D6 effector P14-gfp cells were incubated *in vitro* with infection-matched tissue for 1-3h before 2-photon microscopy. Still images from video with third dimension flattened show P14 cells (white arrowhead) under

the collagen capsule layer, Scale bar=50μm. (F) Congenically marked D6 effector (11×10^6) and naïve (1.61×10^6) P14 CD8 T cells were mixed and co-transferred i.p. into infection matched recipients. PBL was taken at indicated time points after injection. (G) D6 effector P14 were transferred i.p. into D6 LCMV infection matched or naïve recipients. 3h after injection, tissues were harvested and analyzed for attachment of transferred cells. (H) Representative images of D6 effector P14 cells adhered to spleen and kidney, scale bar=100μm(left) or 50μm (right). Graph shows mean and SEM, ***$p<0.0001$, **p 0.0012, Mann-Whitney test. n= at least 6 from 2-3 separate experiments.

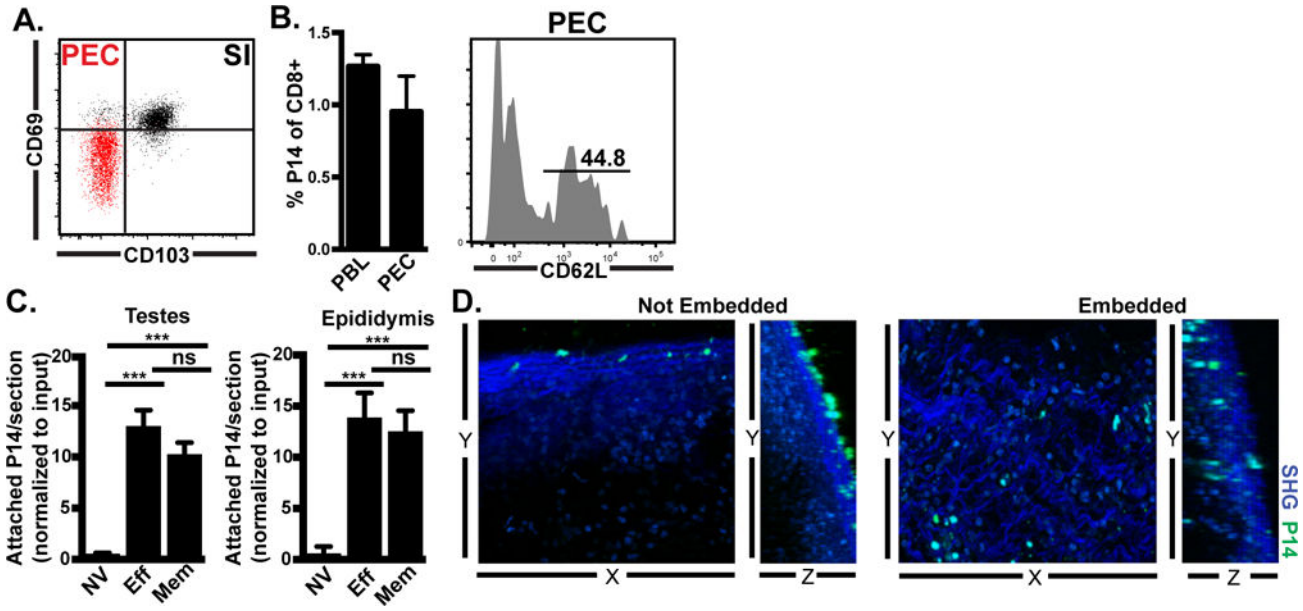

FIGURE 3. Recirculation through peritoneal cavity by memory CD8 T cells allows adherence and transcapsular migration to infected tissues

(A) CD69 and CD103 on gated memory P14 CD8 T cells isolated from small intestine epithelium (SI, black) or peritoneal exudate cells (PEC, red). (B) Memory P14 CD8 T cells isolated from lymphoid organs were transferred i.v. into naïve mice. Donor cells were assessed in recipient blood (PBL) and peritoneal lavage (PEC) 18h later. (C) Naïve (NV), effector (Eff, 6 days after LCMV infection) or memory (Mem, 30 days after LCMV infection) congenically distinct P14 populations were isolated from spleen and co-injected i.p. (4-7.5×10^6 of each cell type) into day 6 LCMV recipients. 3h later, attached P14 were quantified by immunofluorescence. Graph shows mean and SEM and results of Wilcoxon matched pairs statistical analysis, ***p 0.0005, ***p 0.001. (D) Memory P14 CD8 T cells were co-cultured for 2-3h with MGT freshly isolated from LCMV D6 mice. Live imaging was captured by 2-photon microscopy (representative still images shown). n=3 from 2 separate experiments.

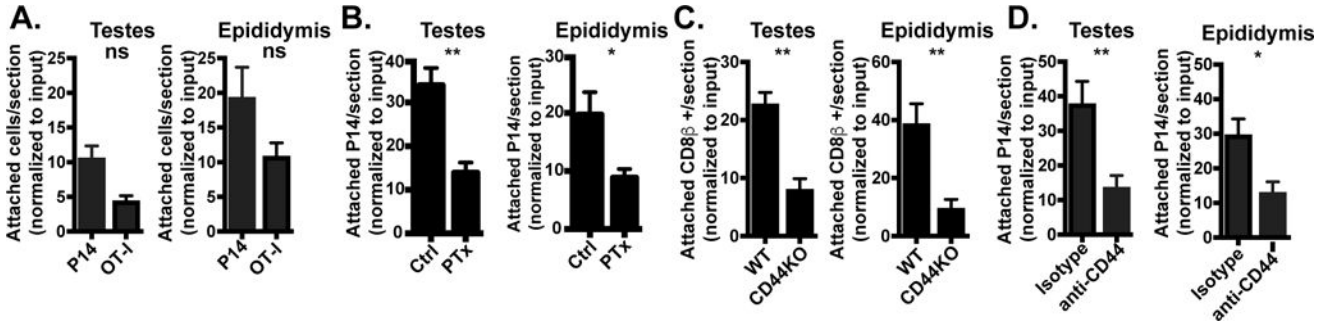

FIGURE 4. Antigen-independent, CD44-dependent mechanism of visceral immunosurveillance

(A) Congenically marked effector P14 (4×10^6) and OT-I (7×10^6) CD8 T cells from day 6 post infection with LCMV and VSV-OVA immune chimeras, respectively, were co-injected i.p. into LCMV infection-matched recipients. 3h after i.p. injection, adhered P14 and OT-I were quantified by immunofluorescence. n=4, representative of n=9 from 2 independent experiments. (B) Effector P14 cells from day 6 LCMV immune chimeras were untreated (Ctrl) or treated with pertussis toxin (PTx) *in vitro* then injected ($4\text{-}12\times10^6$ cells) i.p. into day 6 LCMV infection-matched hosts. 3h later, adhered P14 cells were quantified by immunofluorescence. n=6 from 2 independent experiments. Graphs show mean and SEM. Mann-Whitney statistical analysis, $^{**}p$ 0.0043, $^{*}p$ 0.0260. (C) 6 days after LCMV infection, lymphocytes from WT or CD44KO mice were injected i.p. into WT infection matched recipients. 3h after i.p. injection, adhered CD8β+ transferred cells were quantified by immunofluorescence. n=8 representative of 2 separate experiments. Graphs show mean and SEM. Wilcoxon statistical analysis, $^{**}p$ 0.0043. (D) $4\text{-}9\times10^6$ day 6 effector P14 were untreated or treated with anti-CD44 antibody *in vitro* for 1h prior to i.p. injection into untreated or hyaluronidase treated LCMV infection-matched recipients, respectively. 3h later, adhered P14 were quantified by immunofluorescence. n=6 from 2 separate experiments. Graphs show mean and SEM. Mann-Whitney statistical analysis, $^{**}p$ 0.0027, $^{*}p$ 0.0116.